

E. Lerche, V. Bobkov, P. Jacquet, M.-L. Mayoral, A. Messiaen, I. Monakhov,
J. Ongena, G. Telesca, D. Van Eester, R. R. Weynants
and JET EFDA contributors

Recent Experiments on Alternative Dipole Phasing with the JET A2 ICRF Antennas

“This document is intended for publication in the open literature. It is made available on the understanding that it may not be further circulated and extracts or references may not be published prior to publication of the original when applicable, or without the consent of the Publications Officer, EFDA, Culham Science Centre, Abingdon, Oxon, OX14 3DB, UK.”

“Enquiries about Copyright and reproduction should be addressed to the Publications Officer, EFDA, Culham Science Centre, Abingdon, Oxon, OX14 3DB, UK.”

The contents of this preprint and all other JET EFDA Preprints and Conference Papers are available to view online free at www.iop.org/Jet. This site has full search facilities and e-mail alert options. The diagrams contained within the PDFs on this site are hyperlinked from the year 1996 onwards.

Recent Experiments on Alternative Dipole Phasing with the JET A2 ICRF Antennas

E. Lerche¹, V. Bobkov², P. Jacquet³, M.-L. Mayoral³, A. Messiaen¹, I. Monakhov³,
J. Ongena, G. Telesca, D. Van Eester, R. R. Weynants
and JET EFDA contributors*

JET-EFDA, Culham Science Centre, OX14 3DB, Abingdon, UK

¹LPP, Association "EURATOM – Belgian State", TEC, - Ecole Royale Militaire, B-1000 Brussels Belgium

²MPI für Plasmaphysik, Boltzmannstr. 2, D-85748, Garching, Germany

³EURATOM-UKAEA Fusion Association, Culham Science Centre, OX14 3DB, Abingdon, OXON, UK

* See annex of F. Romanelli et al, "Overview of JET Results",
(Proc. 22nd IAEA Fusion Energy Conference, Geneva, Switzerland (2008)).

Preprint of Paper to be submitted for publication in Proceedings of the
18th Topical Conference on Radio Frequency Power in Plasmas, Gent, Belgium.
(22nd June 2009 - 24th June 2009)

ABSTRACT.

Using the JET A2 ICRF antennas [1], experiments were carried out to assess the performance of three different dipole phasing configurations relevant for the operation of the ICRF antenna in ITER. Three similar discharges with dipole ($0\pi0\pi$), “symmetric dipole” ($0\pi\pi0$) and “super dipole” ($00\pi\pi$) phasings were compared. In the “super dipole” case, higher coupling was confirmed but lower heating efficiency and much stronger plasma wall interaction were observed, as corroborated, respectively, by the analysis of the diamagnetic energy response to the ICRF power steps and by the observation of a considerable temperature rise of the antenna limiters and septa in the $00\pi\pi$ case. These observations were found to be in line with simulations of the ICRF wave absorption and with High Frequency Structure Simulator (HFSS) modeling of the RF fields near the antenna [2].

1. INTRODUCTION

The main difficulty of Ion Cyclotron Radio Frequency (ICRF) heating schemes in large tokamaks comes from the fact that the fast waves launched by the antenna have to cross a region of low density – where the waves are typically evanescent – before reaching the main plasma. The wider this region the lower the antenna coupling and consequently less power can be effectively coupled to the plasma for a given voltage applied to the antenna. The amount of RF power that can tunnel through the evanescence region depends on the decay length of the wave excited. For a given RF frequency, waves with smaller parallel wave components k_{\parallel} are less evanescent than waves with larger k_{\parallel} and therefore different antenna phasings (leading to different k_{\parallel} spectra excited) are expected to show different coupling properties. On the other hand, the wave absorptivity increases with k_{\parallel} and thus the overall performance of an ICRF system depends on a compromise of producing an antenna excitation with low enough k_{\parallel} to ensure an acceptable plasma coupling but with high enough k_{\parallel} to still feature satisfactory ICRF absorption [3]. The dependence of the ICRF efficiency on the antenna phasing in the JET tokamak was already studied in the past [4-6]. One of the conclusions was that the installation of central septa in the A2 antenna arrays changed the coupling / absorption properties considerably for the low k_{\parallel} spectra. During the last experimental campaign at JET, the performance of three dipole phasings of the A2 antennas was readdressed. The main results of these experiments are reported below.

2. EXPERIMENTAL OBSERVATIONS

The experiments were performed in L-mode with a magnetic field of $B_0 = 3\text{T}$, a plasma current of $I_p = 2\text{MA}$, a central density of $n_{e0} = 3.5 \times 10^{19} \text{m}^{-3}$ and an antenna-separatrix distance of $11.0 \pm 0.5\text{cm}$. Minority hydrogen ICRF heating at $f = 42\text{MHz}$ was used with $\sim 7\%$ of H and about 4MW ICRF power was applied. In Fig.1 various quantities of three similar discharges with $0\pi0\pi$, $0\pi\pi0$ and $00\pi\pi$ antenna phasings are compared.

First note that despite the fact that the loading (g) is higher for the $00\pi\pi$ pulse, the other two discharges exhibit much higher heating efficiency, as clearly seen on the larger values of electron

temperature (c), diamagnetic energy (d) and neutron rate (e) reached after the RF power is applied. The heating efficiencies inferred from break-in-slope analysis of the plasma diamagnetic energy response are $\eta = 0.85 \pm 0.1$, $\eta = 0.8 \pm 0.1$ and $\eta = 0.54 \pm 0.1$ for the pulses with $0\pi 0\pi$, $0\pi\pi 0$ and $00\pi\pi$ phasings, respectively. Also note that, in spite of the somewhat lower bulk plasma density, the radiation losses in Pulse No: 74091 are larger, indicating a higher level of impurities in the plasma. This observation is also supported by spectroscopic measurements at the plasma edge.

Another striking difference between the $00\pi\pi$ discharge and the other two pulses is depicted in Fig.1(h), where the time traces of the temperature measured by an Infra-Red (IR) camera [7] on the equatorial region of the central septum of antenna B are compared. The surface temperature for the pulse with $00\pi\pi$ phasing overcomes 800°C while the temperature during the two other discharges lies around 400°C . As a matter of fact, the antenna septa and close limiters reach the highest surface temperatures in Pulse No: 74091 and a ‘bright spot’ was observed in the visible camera close to antenna B, although the plasma equilibrium and the ICRF power was similar for the 3 discharges.

This stronger plasma-wall interaction observed in Pulse No: 74091 is related to enhanced excitation of coaxial modes and to larger RF sheath rectification, i.e. to the fact that the net parallel RF electric field excited close to the antenna is larger for the $00\pi\pi$ phasing configuration than for the other two cases and non-resonant acceleration of charged particles in the edge / SOL is enhanced. Numerical modelling of the A2 antennas using HFSS confirms that the near fields and the image currents excited in the antenna box are indeed larger in the super-dipole case, as discussed in detail in [2].

3. MODELLING

The ICRF power spectra excited by the A2 antennas computed with the ANTITER code [8] using the main parameters of the experiments are shown in Fig.2(a) for the 3 different dipole phasings discussed: $0\pi 0\pi$ (solid), $0\pi\pi 0$ (dashed) and $00\pi\pi$ (dash-dotted). The spectra were normalized to produce the same total power for all cases.

Note that in the standard dipole configuration ($0\pi 0\pi$) roughly 80% of the power is launched around $|k_{\parallel}| \approx 6.5\text{m}^{-1}$ whereas the super-dipole phasing ($00\pi\pi$) has ~90% of the power associated to lower $|k_{\parallel}| \approx 2.5\text{m}^{-1}$ values and hence features higher coupling (Fig.1(g)). The double-pass absorption efficiency computed with the 1D ICRF TOMCAT code [9] for the experimental conditions of the studied pulses is plotted in Fig.2(b) as function of the k_{\parallel} wave-numbers considered. In these simulations, the fast wave is launched from a propagative region inside the plasma and thus coupling properties and edge/SOL losses are not described. Moreover, being a 1D (radial) code, TOMCAT does not include the excitation of coaxial modes in the torus nor the asymmetry in the k_{\parallel} spectrum absorption caused by poloidal field effects. Despite the simplicity of the model, these results already shed some light on the different heating performances seen experimentally. In the $0\pi 0\pi$ and $0\pi\pi 0$ discharges, a fair fraction of the power is launched in a k_{\parallel} range where the wave absorption is quite efficient while the $00\pi\pi$ phasing launches the ICRF power in a k_{\parallel} range where the double-pass absorption is small (due to the narrower ICRF absorption region of the low k_{\parallel} waves). The heating

efficiencies estimated by convoluting the absorptivity given by TOMCAT with the antenna spectra shown in Fig.2(a) $\int |j_{ant}|^2 \mu(k_{\parallel}) dk_{\parallel}$, are indicated in the legend.

The values for the $0\pi 0\pi$ and $0\pi\pi 0$ phasings are in fair agreement with the experimental results while the heating efficiency for the $00\pi\pi$ case is somewhat underestimated. This comes from the fact that in this simplified model it is considered that the power that is not absorbed in a double-pass is lost, which is probably a too strong assumption for the low absorptivity cases. 3D full-wave modelling describes the antenna coupling as well as the excitation of coaxial modes is ongoing.

SUMMARY

Three similar JET discharges with different ICRF dipole antenna phasings were described. As expected, the “super-dipole” $00\pi\pi$ phasing, which privileges the excitation of waves with low k_{\parallel} values, features higher plasma coupling than the other two studied phasings ($0\pi 0\pi$ and $0\pi\pi 0$). For this phasing configuration, however, it was observed that the heating efficiency was significantly lower and that the plasma-wall interactions were strongly enhanced. The latter is mainly attributed to enhanced excitation of coaxial modes and to higher net parallel electric fields due to RF sheath rectification close to the antennae, which enhance parasitic RF dissipation in the scrape-off layer. 1D modelling of the ICRF wave absorption including the toroidal spectra excited in each phasing configuration corroborates the different heating efficiencies observed experimentally.

ACKNOWLEDGEMENTS

The authors would like to thank R. Koch and P. Lamalle for their input to this work.

REFERENCES

- [1]. A. Kaye et al., *Fusion Eng. and Design* **74** (1994) p.1-21
- [2]. V. Bobkov et al., invited talk at this conference
- [3]. R. Weynants et al., review talk at this conference
- [4]. A. Kaye et al., Fusion Engineering 1995 SOFE, 16th IEEE/NPSS Symposium **V1**, PP.736-741
- [5]. D. D’Ippolito et al., AIP Conf. Proc **59** (2001) p.114
- [6]. J. Heikkinen et al., Proc. of 31st EPS Conf. on Plasma Physics 2004 (London) ECA **28B** P 5.162
- [7]. E. Gauthier et al., *Fusion Eng. and Design* **82** (2007) p. 1335
- [8]. P.U. Lamalle et al., *Nucl. Fusion* **46** (2006) p.432
- [9]. D. Van Eester and R. Koch, *Plasma Physics Contrl. Fusion* **40** (1998) p.1949

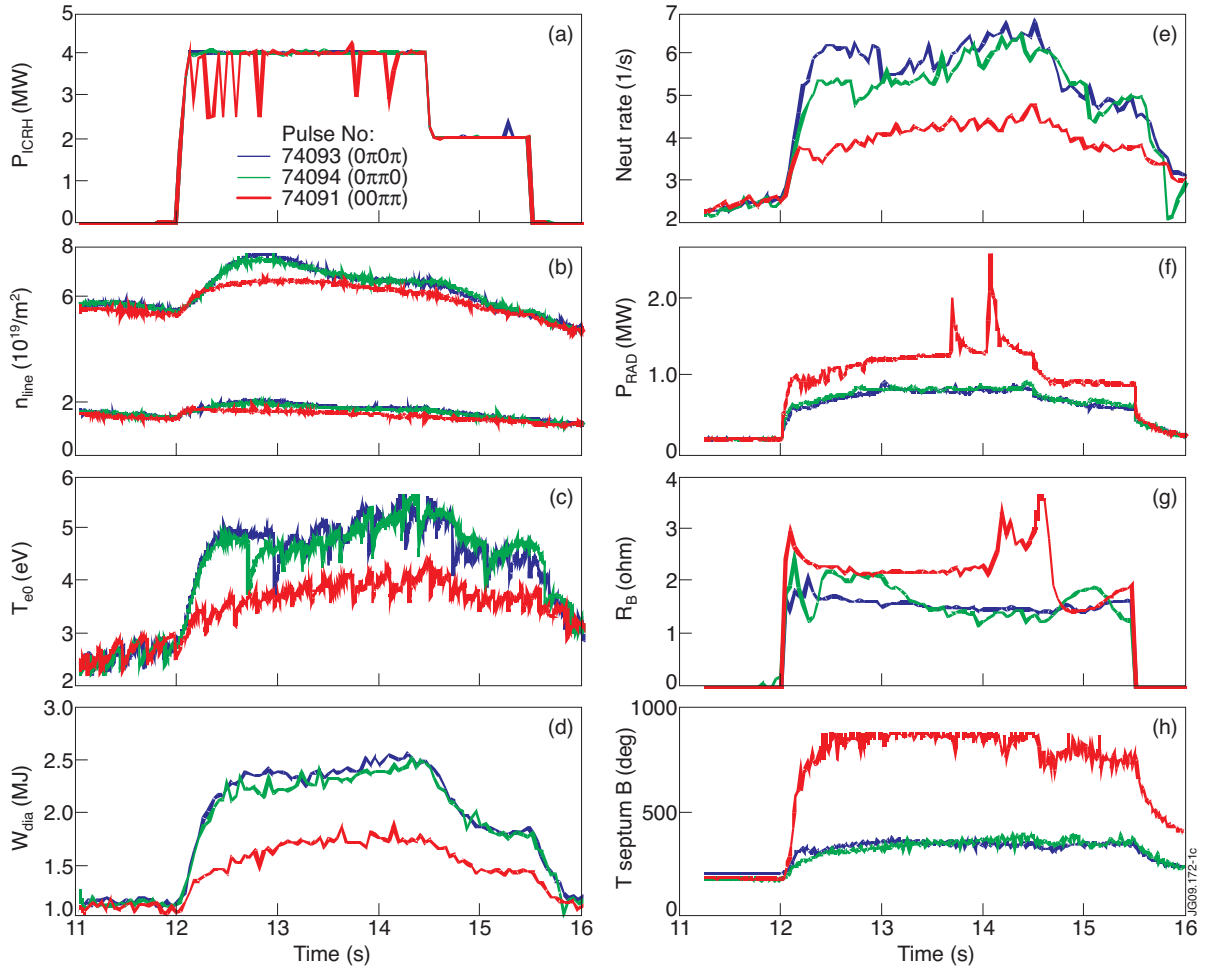


Figure 1: Comparison of 3 similar plasma discharges with $0\pi0\pi$ (Pulse No: 74093), $0\pi\pi0$ (Pulse No: 74094) and $00\pi\pi$ (Pulse No: 74091) ICRF antenna phasings; (a) Total ICRF power (A+B+C), (b) line integrated densities, (c) central electron temperature, (d) diamagnetic energy, (e) total neutron rate, (f) total radiated power, (g) strap-averaged coupling resistance of antenna B, (h) surface temperature of septum B (from IR camera).

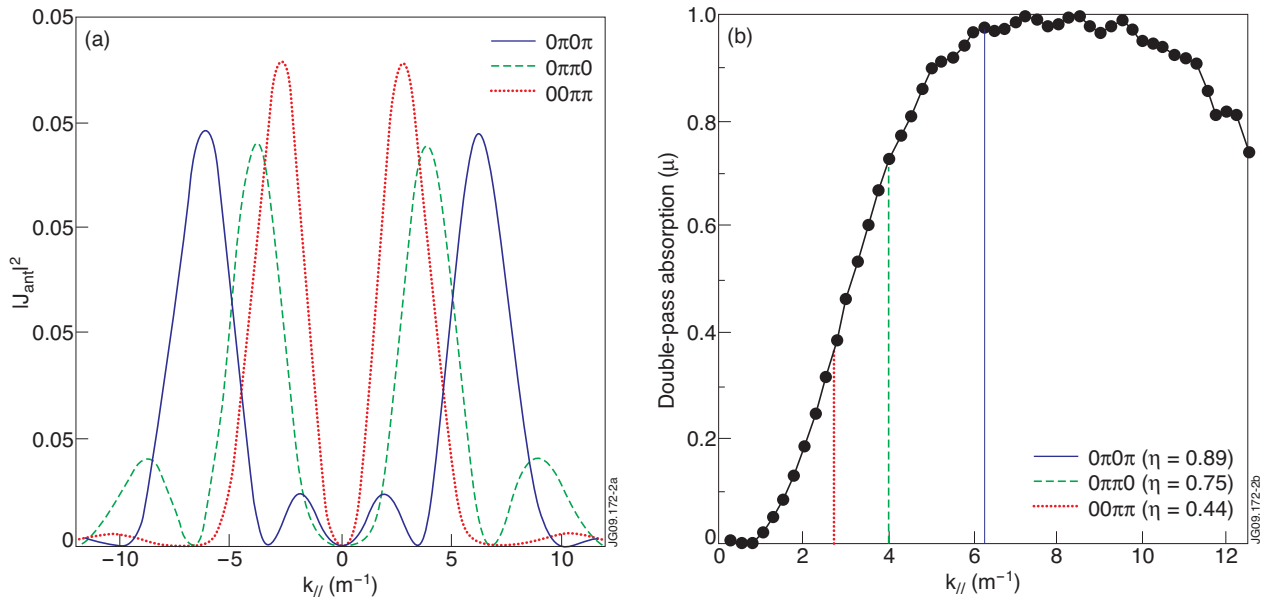


Figure 2: (a) Power density spectra of the A2 antennas with 3 different current phasings: $0\pi0\pi$ (solid), $0\pi\pi0$ (dashed) and $00\pi\pi$ (dot-dashed); (b) Double-pass absorption efficiency computed with the 1D TOMCAT wave code as function of the $k_{||} = N/R$ wave-number launched.